

Non-minimal Lorentz invariance violation in light of muon anomalous magnetic moment and long-baseline neutrino oscillation data

Hai-Xing Lin,^{*} Jian Tang,[†] and Sampsa Vihonen[‡]
School of Physics, Sun Yat-sen University, Guangzhou 510275, China

Pedro Pasquini[§]
Tsung-Dao Lee Institute (TDLI), Shanghai Jiao Tong University (SJTU), Shanghai 200240, China
(Dated: May 17, 2022)

In light of the increasing hints of new physics at the muon $g - 2$ and neutrino oscillation experiments, we consider the recently observed tension in the long-baseline neutrino oscillation experiments as a potential indication of Lorentz invariance violation. For this purpose, the latest data from T2K and NO ν A is analysed in presence of non-minimal Lorentz invariance violation. Indeed, we find that isotropic violation in dimensions $D = 4, 5$ and 6 can alleviate the tension in neutrino oscillation data by about $0.4\text{--}2.4\sigma$ CL significance, with the isotropic coefficient $\gamma_{\tau\tau}^{(5)} = 3.58 \times 10^{-32} \text{GeV}^{-1}$ yielding the best fit. At the same time, the anomalous muon $g - 2$ result can be reproduced with an additional non-isotropic violation of $d^{zt} = -1.7 \times 10^{-25}$. The analysis highlights the possibility of simultaneous relaxation of experimental tensions with Lorentz invariance violation of mixed nature.

I. INTRODUCTION

Standard Model (SM) of particle physics is the most successful theory to describe properties of elementary particles and their interactions. Its robustness has been tested in numerous experiments, culminating in the discovery of Higgs boson at the LHC. The conservation of Lorentz invariance and CPT symmetry are an inseparable part of SM physics, as they ensure that physics stay the same regardless of the observer. Only recently, the integrity of SM has started to falter as mounting evidence from electroweak precision observables, CKM matrix element measurements and neutrino experiments are showing divergences between experiments and SM predictions. As physicists look for methods to accommodate SM physics in a more complete theoretical framework, searching evidence of violation to fundamental symmetries could provide hints of the underlying theory, such as the formulation of quantum gravity [1–3].

CPT is a fundamental symmetry that is conserved in quantum field theories set in a flat spacetime [4, 5]. It is closely related to Lorentz invariance [6]. Well-known examples of theories that give rise to Lorentz Invariance Violation (LIV) or CPT violation are found in the string theory [7, 8], while LIV could also arise in supersymmetry together with CPT violation [9] and even without it [10]. An example of a simple non-local field theory of CPT violation can be found in Ref. [11]. Generally speaking, theories that uphold any non-trivial space-time dependence on the vacuum also lead to violation of either Lorentz invariance, CPT symmetry, or both. Lorentz invariance can furthermore be violated isotropically or into

a specific direction. Effects of LIV and CPT violation are typically studied in the effective field theory framework, the most general one being the famous Standard Model Extension [12] where SM Hamiltonian is expanded to arbitrary dimensions. Evidence of LIV or CPT -odd operators have been searched in many experiments from atmospheric neutrino fluxes to gravitational waves [13–17], which have led to very stringent constraints especially for high-order operators [18, 19].

In this work, we study the prospects of uncovering LIV physics in neutrino oscillation experiments. Neutrino oscillations stand out as the first direct evidence of physics beyond SM, making neutrino experiments an ideal platform to look for new physics. In recent years, significant advances have been made in the precision measurements of the standard oscillation parameters: θ_{13} has been measured at a few-percent-level at 90% confidence level (CL) in reactor experiments, θ_{23} and $|\Delta m_{31}^2|$ in atmospheric and long-baseline neutrino experiments, and θ_{12} and Δm_{21}^2 in a combination of solar and reactor neutrino experiments [20]. At the same time, observations of neutrino anomalies and tensions in oscillation data [21–24] have seeded an intense discussion over whether new physics is in play [25–28]. We investigate the tension in the long-baseline neutrino experiments T2K and NO ν A [29, 30], where recent data has shown contradicting results on the parameters θ_{23} and δ_{CP} . We study the parameter discrepancies in T2K and NO ν A data in light of non-minimal LIV, focusing on the lesser constrained dimensions 4, 5 and 6. It is shown in this work that that isotropic LIV could notably alleviate the tension observed in the three-neutrino mixing. We also show how the recent muon $g - 2$ measurements [31] could simultaneously arise from the LIV operators when non-isotropic coefficients are present.

This article is organized as follows: In section II, we provide a brief overview of the theoretical formalism of LIV effects in neutrino oscillations and muon $g - 2$. In

^{*} linhx55@mail2.sysu.edu.cn

[†] tangjian5@mail.sysu.edu.cn

[‡] sampsa@mail.sysu.edu.cn

[§] ppasquini@sjtu.edu.cn

section III, we describe the experimental data and numerical methods adopted in this work. The results on fitting LIV coefficients into T2K and NO ν A data are presented in section IV. We leave the concluding remarks in section V.

II. LORENTZ INVARIANCE VIOLATION IN NEUTRINO OSCILLATIONS

In this section, we review the theoretical framework to study LIV in neutrino oscillations. We first consider the isotropic LIV effects in section II A. The non-isotropic implementation of LIV is then presented in section II B. Finally, we discuss the implications to LIV coefficients from recent muon $g - 2$ measurements in section II C.

A. Isotropic violation

In the following, we summarize the effective Hamiltonian describing neutrino oscillations under Lorentz invariance violation. The method described in this section was originally proposed in [18] and further developed in [32–34]. We focus on LIV terms that appear in the kinetic term. The generalized kinetic term of the neutrino Lagrangian can be written as

$$\mathcal{L}_D = i\nu_{iL}^\dagger \bar{\sigma}^\mu \partial_\mu [\delta_{ij} - i^{D-4} \gamma_{ij}^{\mu_1 \dots \mu_{D-4}} \partial_{\mu_1} \dots \partial_{\mu_{D-4}}] \nu_{jL} \quad (1)$$

where $\gamma_{ij}^{\mu_1 \dots \mu_{D-4}}$ are tensors of rank $D - 4$ that parametrizes the size of the LIV and σ^μ are the Pauli matrices.

In this work, we mainly focus on the isotropic part of the Lorentz violation. The isotropic sector is generally confined by less stringent bounds [19], which makes it more interesting to probe in experiments. Hence, we will set $\mu_i = 0$ unless stated otherwise. Under the isotropic hypothesis, there is no violation related to direction of the momentum and the neutrino propagation Hamiltonian can therefore be written by two terms, that is,

$$H = H_0 + H_{\text{LIV}}, \quad (2)$$

where H_0 stands for the standard Hamiltonian consistent with SM and H_{LIV} contains the Lorentz-violating terms. In the flavour basis, the standard Hamiltonian is given by $H_0 = U^\dagger \text{diag}[0 \Delta m_{21}^2/2E, \Delta m_{31}^2/2E]U + V(x)$ and LIV part by

$$H_{\text{LIV}} = \begin{pmatrix} \gamma_{ee}^{(D)} & \gamma_{e\mu}^{(D)} & \gamma_{e\tau}^{(D)} \\ \gamma_{e\mu}^{(D)*} & \gamma_{\mu\mu}^{(D)} & \gamma_{\mu\tau}^{(D)} \\ \gamma_{e\tau}^{(D)*} & \gamma_{\mu\tau}^{(D)*} & \gamma_{\tau\tau}^{(D)} \end{pmatrix} E^{D-3}, \quad (3)$$

where we simplified our notation to $\gamma_{\alpha\beta}^{0\dots 0} = \gamma_{\alpha\beta}^{(D)}$. The parameters $\gamma_{\alpha\beta}^{(D)}$ have mass dimension $4 - D$. They are CPT -odd when D is odd and CPT -even when D is even. The corresponding Hamiltonian for antineutrinos

receives a minus sign when D is an odd number. Parameters $\gamma_{\ell\ell}^{(D)}$ ($\ell = e, \mu, \tau$) are real and $\gamma_{\ell\ell'}^{(D)}$ ($\ell \neq \ell'$) are complex parameters with phases $\phi_{\ell\ell'}^{(D)}$. In the following, we mainly study LIV parameters in the flavour basis where $\gamma_{\ell\ell'}^{(D)} = |\gamma_{\ell\ell'}^{(D)}| e^{-i\phi_{\ell\ell'}^{(D)}}$.

B. Non-isotropic violation

In case of non-isotropic Lorentz invariance violation, the strength of LIV effect depends on the direction of the propagating neutrino. In such case, the equation of state can be decomposed into two parts [35]:

$$[i\delta_{\alpha\beta}\partial_t - H_0 - \delta H] \nu_\beta = 0, \quad (4)$$

where H_0 conserves Lorentz invariance and δH violates it. Assuming the neutrino propagates into direction \mathbf{x} , the conserving part can be written as

$$H_0 = -\gamma^0 (i\delta_{\alpha\beta}\boldsymbol{\gamma} \cdot \nabla_{\mathbf{x}} - M_{\alpha\beta}), \quad (5)$$

where the neutrino mass matrix is given by $M_{\alpha\beta}$ ($\alpha, \beta = e, \mu, \tau$). The perturbation introducing Lorentz invariance violation on the other hand can be presented as

$$\delta H = -\frac{1}{2} d_{\alpha\beta}^{\mu 0} (\gamma^0 \gamma_5 \gamma_\mu H_0 + H_0 \gamma^0 \gamma_5 \gamma_\mu) - i d_{\alpha\beta}^{\mu j} \gamma^0 \gamma_5 \gamma_\mu \partial_j, \quad (6)$$

where $d_{\alpha\beta}^{\mu j}$ is the strength of the Lorentz violation into the direction \vec{x}_j ($j = 1, 2, 3$). We assume neutrino propagation align with direction \vec{x}_3 and keep only the axial-current operator related to $\gamma_5 \gamma_\mu$. As we shall see in the following section, parameter $d_{\alpha\beta}^{\mu j}$ could have profound implications in the calculation of muon anomalous magnetic moment.

In order to derive the evolution equation for neutrinos, the neutrino mass matrix M must be diagonalized. This can be accomplished within the relativistic limit $|\mathbf{p}| \gg m_i$, where $p_\mu \approx (|\mathbf{p}|, -\mathbf{p})$. In such a case the evolution equation is given by [36]

$$i\partial_t \psi_i = \left(|\mathbf{p}| + \frac{m_i^2}{2|\mathbf{p}|} - \frac{1}{|\mathbf{p}|} d_{\alpha\beta}^{\mu\nu} p_\mu p_\nu \right) \psi_i \quad (7)$$

where ψ_i is the mass eigenstate of the Hamiltonian $H = H_0 + \delta H$. It is also convenient to express coordinates in the Sun-centered inertial frame [35],

$$i\partial_t \psi_i = \left(|\mathbf{p}| + \frac{m_i^2}{2|\mathbf{p}|} - d_{ij}^{zt} |\mathbf{p}| \cos \Theta \right) \psi_i, \quad (8)$$

where Θ denotes colatitude [37] of the Earth. Neutrino experiments with large variation in colatitude can therefore provide sensitive probes to LIV of this kind.

In neutrino oscillations, we introduce non-isotropic LIV to oscillation probabilities. To do this, we include the non-isotropic coefficient d^{zt} from equation (8) in addition to the isotropic LIV parameters $\gamma_{\ell\ell'}^{(D)}$ in the Hamiltonian (3).

C. Implications of $(g-2)_\mu$ measurement

In this subsection, we calculate the contribution to anomalous muon magnetic moment from Lorentz invariance violation. It was recently reported by $g-2$ col-

$$\mathcal{L}_{LIV} = \bar{\mu} \left[-a_\mu \gamma^\mu + b_\mu \gamma_5 \gamma^\mu + \frac{i}{2} c^{\alpha\beta} \gamma_\alpha D_\beta + \frac{i}{2} d^{\alpha\beta} \gamma_5 \gamma_\alpha D_\beta - \frac{1}{2} H^{\alpha\beta} \sigma_{\alpha\beta} \right] \mu \quad (9)$$

where a_α , b_α , $c^{\alpha\beta}$, $d^{\alpha\beta}$ and $H^{\alpha\beta}$ parameterize LIV for muons and $D^\alpha = \partial^\alpha + A^\alpha$ is the covariant derivative. Whereas a_α and b_α are *CPT*-odd, other coefficients are *CPT*-even. Most of these parameters are strictly constrained by previous experiments [19].

The general contribution to the muon $g-2$ frequency is given by [39]

$$\delta\omega^\pm = 2 \sum_{dnjm} E^{D-3} e^{im\omega_\oplus t} G_{jm} \left[\check{H}_{nlm}^{(D)} \pm \check{g}_{nlm}^{(D)} \right], \quad (10)$$

where E^{D-3} denotes neutrino energy in dimension $D = 3, 4, 5, \dots$, ω_\oplus is the Earth's frequency around the Sun and factors \check{H}_{nlm}^D and \check{g}_{nlm}^D are combinations of parameters b_μ , $d^{\alpha\beta}$ and $H_{\alpha\beta}$. Function $G_{jm} = G_{jm}(\Theta)$ on the other hand depends on colatitude Θ and vanishes for the isotropic case $j = 0$. LIV must therefore be non-isotropic to explain the anomalous muon $g-2$ value.

In case of non-isotropic LIV, the contribution to muon $g-2$ arises from mass dimension $D = 5$. When $j = 1$, $m = 0$, the G_{jm} function yields

$$\delta\omega = -2 \frac{E^2}{m_\mu} G_{10} \sqrt{\frac{4\pi}{3}} d^{zt} = -2 \frac{E^2}{m_\mu} d^{zt} \cos \Theta, \quad (11)$$

where $G_{10}(\Theta) = 0.5\sqrt{3/\pi} \cos \Theta$. The total correction to SM value of muon magnetic moment a_μ is therefore

$$\Delta a_\mu = -\frac{2E^2 \cos \Theta}{eB} d^{zt}, \quad (12)$$

where B is the magnetic field. The $g-2$ collaboration [31] reported the value of $\Delta a_\mu = 251 \times 10^{-11}$ in their recent measurement, which was acquired in magnetic field $B = 1.45$ T and colatitude $\Theta = 48.2^\circ$ [40]. This correction to muonic $g-2$ can be also obtained with non-isotropic LIV coefficient $d^{zt} = -1.7 \times 10^{-25}$ from equation (12). Such a coefficient is well within the present experimental bounds from the neutrino sector [19]. For more details about the $g-2$ measurement, see also Refs. [41–45].

III. DESCRIPTION OF THE NEUTRINO OSCILLATION DATA

In the present work, we focus on the analysis of the neutrino oscillation data from the presently running

laboration that the muon magnetic moment is different from the Standard Model prediction by 4.2σ CL [31]. We show in the following that this value can be accommodated with the non-isotropic LIV coefficient d_{zt} in mass dimension $D = 5$.

The general Lagrangian responsible for LIV in muonic sector can be written as [38]

Tokai-to-Kamioka (T2K) and NuMI Off-axis ν_e Appearance (NO ν A) experiments. T2K and NO ν A are long-baseline accelerator based experiments where intensive beams of neutrinos and antineutrinos are created by colliding protons on a fixed target. In this work, we focus on the recent data releases from the T2K and NO ν A collaborations reported in Refs. [29] and [30], respectively. A particular area of interest is the observed discrepancy in the θ_{23} measurement, which has shown a tension in neutrino oscillation data between T2K and NO ν A according to an analysis in the standard neutrino mixing picture. In this section, we briefly review the experimental data and the analysis methods that are used in our work.

A. T2K experiment

Tokai-to-Kamioka (T2K) experiment is one of the two presently running long-baseline neutrino oscillation facilities. T2K uses a proton accelerator of 750 kW average output to generate muon neutrino and antineutrino beams. Based on the J-PARC campus in Tokai, Japan, the neutrino beam traverses 295 km away to Kamioka, where it is met by SuperKamiokande neutrino detector. The neutrino beam is also monitored at the near and intermediate detector facilities ND280 and INGRID, respectively. Super-Kamiokande and ND280 are both located 2.5° off the beam axis, where the observed neutrinos are mainly of about 600 MeV energy. The beam polarity can be switched between muon neutrino and antineutrino modes, with the initial strategy of dividing the operational time into 2 years in neutrino mode and 6 years in antineutrino mode, respectively. A second run is planned for T2K experiment (T2K-II), with the aim to continue the successful run of the first stage.

The neutrino beam used in T2K consists predominantly of muon neutrinos (96%–98%), accompanied by smaller components of beam-related backgrounds. The corresponding antineutrino beam has similar composition with muon antineutrinos taking the majority. Most neutrinos and antineutrinos interact via charged-current quasi-elastic (CCQE) interaction with a small but observable chance for resonant charged-current pion pro-

duction ($CC1\pi$). The neutrino data collected in SuperKamiokande is typically reported in five different samples: two appearance channels measuring $\nu_\mu \rightarrow \nu_e$ and $\bar{\nu}_\mu \rightarrow \bar{\nu}_e$ oscillations via CCQE interaction and two disappearance channels $\nu_\mu \rightarrow \nu_\mu$ and $\bar{\nu}_\mu \rightarrow \bar{\nu}_\mu$. There is also a third appearance channel dedicated to $\nu_\mu \rightarrow \nu_e$ oscillations observed via $\nu_e CC1\pi^+$ interaction. All neutrino events are reconstructed from the information coming from the Cherenkov light when charged particles interact with the water content of the neutrino detectors.

In this work we analyse the neutrino data that has been collected in the first phase of T2K between years 2009 and 2018. In Refs. [29, 46, 47], T2K collaboration reported neutrino oscillation data from 3.13×10^{21} protons-on-target (POT). The collected data contains the information about the reconstructed neutrino and antineutrino events from the combined run of 1.49×10^{21} POT in neutrino beam and 1.64×10^{21} POT in antineutrino beam, respectively. The ν_μ and $\bar{\nu}_\mu$ CCQE samples are divided into 28 and 19 energy bins in the interval [0.2, 3.0] GeV. Correspondingly, ν_e and $\bar{\nu}_e$ CCQE are scattered over 23 same-size energy bins within [0.1, 1.25] GeV interval and $\nu_e CC1\pi^+$ in 16 bins within [0.45, 1.25] GeV respectively. All neutrino and antineutrino events were recorded in SuperKamiokande, which is assumed to have 22.5 kton of fiducial mass.

B. $NO\nu A$ experiment

NuMI Off-axis ν_e Appearance ($NO\nu A$) experiment is the second of the two long-baseline neutrino oscillation experiment currently collecting data. Based in the United States, $NO\nu A$ generates beams of muon neutrinos and antineutrinos and sends them to traverse 810 km underground. The neutrino source is based on the NuMI beamline in Fermilab, Illinois, which produces neutrinos with an average beam power of 700 kW. The detector facilities in $NO\nu A$ are a near detector located 1 km from the beam facility and a far detector stationed at an underground laboratory in Ash River, Minnesota. Both detector facilities are placed 0.8° off-axis from the source. In contrast to T2K, neutrinos and antineutrinos produced in $NO\nu A$ spread over a wide range of energies around 2 GeV. Neutrino interactions observed in $NO\nu A$ therefore consist of various types of charged-current (CC) interactions.

The neutrino and antineutrino data analyzed in this work is based on the events that were collected in $NO\nu A$ far detector in 2014-2020 [30]. The considered data sets were acquired in the far detector, which is a segmented detector consisting of alternating planes of PVC scintillator. The neutrino detection in $NO\nu A$ is based on scintillation light that is emitted by the charged particles created in neutrino-nucleus interactions. The data consist

of six different samples which correspond to 12.5×10^{20} POT in neutrino mode and 13.6×10^{20} POT in antineutrino modes. There are four electron-like characterising $\nu_\mu \rightarrow \nu_e$ and $\bar{\nu}_\mu \rightarrow \bar{\nu}_e$ oscillations and two muon-like samples describing $\nu_\mu \rightarrow \nu_\mu$ and $\bar{\nu}_\mu \rightarrow \bar{\nu}_\mu$ disappearance. The electron-like samples are assigned into two categories based on the purity of each event: low- CNN_{evt} and high- CNN_{evt} . Here CNN_{evt} stands for the convolutional neural network used in particle identification. The muon-like events are split into 19 unequally spaced energy bins in the range [0.75, 4.0] GeV, whereas the electron-like events are distributed in 6 same-size bins over [1.0, 4.0] GeV interval. There is also the so-called peripheral sample included in $NO\nu A$, which is used to increase the number of pure electron-like events. In this work, we consider the samples for the electron-like, muon-like and peripheral events while assuming 14 kton fiducial mass in the far detector.

C. Numerical analysis

The analysis of T2K and $NO\nu A$ data is based on the χ^2 method. The numerical analysis conducted in this work is done with General Long Baseline Experiment Simulator (GLOBES) [48, 49], which has been modified to calculate neutrino evolution with Lorentz invariance violation. The essential parameters as well as the collected neutrino events are summarized for the T2K and $NO\nu A$ experiments in table I.

The neutrino data is analysed with the following χ^2 function:

$$\chi^2 = \sum_i 2 \left[T_{i,d} - O_{i,d} \left(1 + \log \frac{O_{i,d}}{T_{i,d}} \right) \right] + \frac{\zeta_{\text{sg}}^2}{\sigma_{\zeta_{\text{sg}}}^2} + \frac{\zeta_{\text{bg}}^2}{\sigma_{\zeta_{\text{bg}}}^2} + \text{priors}, \quad (13)$$

where index $i = 1, 2, \dots$ runs over the energy bins. Here O_i and T_i stand for the observed and theoretical (predicted) events in the far detectors of T2K and $NO\nu A$. Nuisance parameters ζ_{sg} and ζ_{bg} are used in the calculation to reflect systematic uncertainties in the signal and background events, respectively. The systematic uncertainties are addressed with the so-called pull-method [50]. The systematic uncertainties considered in this work influence the predicted events T_i in neutrino detectors with a simple shift: $T_{i,d} = (1 + \zeta_{\text{sg}})N_{i,d}^{\text{sg}} + (1 + \zeta_{\text{bg}})N_{i,d}^{\text{bg}}$, where $N_{i,d}^{\text{sg}}$ and $N_{i,d}^{\text{bg}}$ denote the predicted signal and background events, respectively. The prior function is defined as the Gaussian distributions of each of the standard neutrino oscillation parameters.

Calculation of theoretically predicted events T_i is performed entirely by GLOBES. The number of events can be described with the formula

$$T_i = N_{\text{nucl}} T \epsilon \int_{E_{\text{min}}}^{E_{\text{max}}} \int_{E'_{\text{min}}}^{E'_{\text{max}}} dE dE' \phi(E) \sigma(E) R(E, E') P_{\nu_\ell \rightarrow \nu_{\ell'}}(E), \quad (14)$$

TABLE I. Summary of the experimental configurations considered in the numerical analysis. Both experiments describe superbeam configurations of either Water Cherenkov (WC) or Totally Active Scintillator Detector (TASD) technology.

Experiment	T2K	NO ν A
Source location	Japan	USA
Beam power	750 kW	700 kW
Protons-on-target	3.13×10^{21}	12.33×10^{20}
Detector type	WC	TASD
Detector mass	22.5 kt	14 kt
Baseline length	295 km	810 km
Off-axis angle	2.5°	0.8°
Data source	Ref. [29]	Ref. [30]

where properties of the neutrino experiment are integrated over the true energy E and reconstructed energy E' of the incident energy. The first part, $N_{\text{nucl}} T \epsilon$, is independent of energy and is defined by the number of nucleons in the neutrino detector, operational time of the experiment and detector efficiency, respectively. The integrand on the other hand is formed by the neutrino flux $\phi(E)$, cross-section $\sigma(E)$, energy resolution function $R(E, E')$ and oscillation probability $P_{\nu_\ell \rightarrow \nu_{\ell'}}(E)$. In this work, we adopt the neutrino fluxes and cross-sections for T2K and NO ν A from Refs. [51, 52] and [53–55], respectively.

One of very important elements in the analysis of the neutrino oscillation data is the detector response associated with T2K and NO ν A experiments. In the event calculation, the detector response is mainly represented by function $R(E, E')$ which relates the incident and reconstructed neutrino energies E and E' with a Gaussian function of width $\sigma_{\text{res}}(E)$. We analyse the T2K and NO ν A far detector data using a modified energy resolution function, where the Gaussian width is given by $\sigma_{\text{res}}(E) = \alpha E + \beta \sqrt{E}$. We furthermore introduce an additional phase shift γ in detector response function $R(E, E')$. The energy resolution function is determined for T2K and NO ν A by fitting parameters α , β and γ recursively for each channel until the correct spectral shape is achieved. Remaining inconsistencies between the official data and prediction of GLoBES are mitigated with channel and bin-based efficiencies.

In order to compute the probabilities $P_{\nu_\ell \rightarrow \nu_{\ell'}}$ with general Lorentz invariance violation and $l, l' = e, \mu, \tau$, a custom-made probability code is adopted to include the

calculation of isotropic and non-isotropic LIV effects in GLoBES. It should be noted that Lorentz invariance violation of higher dimensions could in principle influence the neutrino fluxes $\phi(E)$. In this work, however, we assume the effect on fluxes to be small and fall within the present uncertainties of the neutrino fluxes.

The systematic uncertainties used in the χ^2 function (13) are one of the key characteristics in the analysis of the neutrino oscillation data. In the analysis of experiment data from T2K experiment, we impose 5% systematic uncertainty on the signal events undergoing CCQE interaction. The corresponding background events are addressed with 10% systematic uncertainty. Identical systematic uncertainties are used for the events associated with CC1 π . This choice of priors for the nuisance parameters are found to reproduce the fit results reported by the T2K Collaboration in Ref. [29] with sufficient accuracy. In a similar manner, we implement systematic uncertainties on the each channel considered in the NO ν A experiment. In the analysis of NO ν A far detector data, systematic uncertainties are driven by detector calibration, which amounts to about 5% systematic uncertainty [30]. We treat electron-like samples with low and high CNN_{evt} with the same pull parameters. The systematic uncertainties used here are found to be adequate to reproduce the official results reported by the NO ν A Collaboration in Ref. [30].

IV. NUMERICAL RESULTS

We present the results of our numerical analysis in this section. In this work, we investigated effects of general Lorentz invariance violation (LIV) in dimensions $D = 4, 5$ and 6 . The effects were studied in the context of the θ_{23} discrepancy recently observed in T2K and NO ν A. In the following, we examine whether LIV could alleviate the observed tension between the recent data in T2K and NO ν A and improve the fit to the standard neutrino oscillation parameters. At the same time, we study the effect of LIV in the anomalous muon magnetic moment. As we shall see in this section, isotropic LIV with dimension $D = 5$ provides the best fit result to the T2K and NO ν A data while its non-isotropic version is simultaneously able to resolve $(g - 2)_\mu$.

We first begin investigation with the isotropic Lorentz invariance violation. The analysis of the T2K and NO ν A far detector data is carried out in dimensions $D = 4, 5$ and 6 . The first goal of this study is to identify the LIV parameters that lead to significant improvement on the goodness-of-fit in the T2K and NO ν A data. The second goal is to determine the resulting effect on the fit values of $\sin^2 \theta_{23}$ and δ_{CP} .

TABLE II. Fit results from the scan of isotropic Lorentz invariance violation in dimension $D = 4, 5$ and 6 . The results are obtained from a combined fit to T2K and NO ν A far detector data. The consequent improvement to the fit is shown in the $\Delta\chi^2$ and significance columns. Results are obtained assuming normal ordering for neutrino masses.

Parameter	Fit value ($\sin^2\theta_{23}$)	Fit value (δ_{CP}/π)	Fit value ($ \gamma_{\ell\ell'} $)	$\Delta\chi^2$	Significance (C.L.)
$\gamma_{ee}^{(4)}$	0.562	1.33	-4.62×10^{-23}	0.89	0.95σ
$\gamma_{e\mu}^{(4)}$	0.562	1.48	0.88×10^{-23}	3.96	1.48σ
$\gamma_{e\tau}^{(4)}$	0.563	1.49	0.95×10^{-23}	4.24	1.56σ
$\gamma_{\mu\mu}^{(4)}$	0.522	1.30	5.58×10^{-23}	2.47	1.57σ
$\gamma_{\mu\tau}^{(4)}$	0.549	1.43	-3.75×10^{-23}	4.80	1.69σ
$\gamma_{\tau\tau}^{(4)}$	0.543	1.22	-2.65×10^{-23}	0.57	0.75σ
$\gamma_{ee}^{(5)}$	0.561	1.48	$-4.65 \times 10^{-32} \text{ GeV}^{-1}$	4.34	2.08σ
$\gamma_{e\mu}^{(5)}$	0.561	1.50	$0.28 \times 10^{-32} \text{ GeV}^{-1}$	3.85	1.45σ
$\gamma_{e\tau}^{(5)}$	0.559	1.49	$1.17 \times 10^{-32} \text{ GeV}^{-1}$	4.41	1.60σ
$\gamma_{\mu\mu}^{(5)}$	0.524	1.31	$-3.32 \times 10^{-32} \text{ GeV}^{-1}$	2.73	1.65σ
$\gamma_{\mu\tau}^{(5)}$	0.560	1.26	$-0.45 \times 10^{-32} \text{ GeV}^{-1}$	0.65	0.36σ
$\gamma_{\tau\tau}^{(5)}$	0.526	1.45	$3.58 \times 10^{-32} \text{ GeV}^{-1}$	5.79	2.41σ
$\gamma_{ee}^{(6)}$	0.562	1.34	$-1.15 \times 10^{-41} \text{ GeV}^{-2}$	1.00	1.00σ
$\gamma_{e\mu}^{(6)}$	0.560	1.43	$0.11 \times 10^{-41} \text{ GeV}^{-2}$	3.05	1.23σ
$\gamma_{e\tau}^{(6)}$	0.560	1.46	$0.31 \times 10^{-41} \text{ GeV}^{-2}$	4.90	1.72σ
$\gamma_{\mu\mu}^{(6)}$	0.548	1.25	$0.81 \times 10^{-41} \text{ GeV}^{-2}$	1.32	1.15σ
$\gamma_{\mu\tau}^{(6)}$	0.554	1.27	$-0.17 \times 10^{-41} \text{ GeV}^{-2}$	1.29	0.64σ
$\gamma_{\tau\tau}^{(6)}$	0.544	1.22	$-0.28 \times 10^{-41} \text{ GeV}^{-2}$	0.15	0.39σ

The analysis of the T2K and NO ν A data is carried out as follows. Using the methods described in section III, the far detector data in the two experiments is fitted with a χ^2 function. We fix the solar parameters θ_{12} and Δm_{21}^2 to their respective best-fit values 33.4° and $7.4 \times 10^{-5} \text{ eV}^2$ following the most recent global fit [20]. We also impose a prior from the reactor experiments: $\sin^2 2\theta_{13} = 0.0857 \pm 0.0046$. The χ^2 distribution is computed for parameters $\gamma_{\ell\ell'}^{(D)} = |\gamma_{\ell\ell'}^{(D)}| \exp(-i\phi_{\ell\ell'}^{(D)})$ keeping one LIV parameter free each time. To see the difference to the standard fit, we also obtain the χ^2 distribution corresponding to the case where all LIV parameters are kept at zero.

The fit results to $\sin^2\theta_{23}$ and δ_{CP} from the joint analysis is T2K and NO ν A data are presented in table II. The LIV parameters $\gamma_{\ell\ell'}^{(D)}$ were analysed one by one in dimensions $D = 4, 5$ and 6 . In each row, the denoted parameter was let to run free in order to obtain the fit result. The resulting improvement to the fit result is listed in the $\Delta\chi^2$ column, where $\Delta\chi^2 = \chi_{SM}^2 - \chi_{LIV}^2$ is calculated from χ^2 values attributed to the standard and LIV-influenced fits, respectively. Finally, the significance column indicates the confidence level (C.L.) at which the fit obtained in presence of the LIV parameter is favoured over the standard fit result. The best fit result is obtained with parameter $\gamma_{\tau\tau}^{(5)}$, which can yield an enhancement of

about 2.4σ C.L. in statistical significance. All results are consistent with the experimental bounds reported in the literature [19], including the stringent bounds from IceCube [56]. The statistical significance is computed using Wilks' theorem [57]. For the caveats concerning the statistical analysis in T2K and NO ν A data, see Ref. [58].

The effects of the Lorentz invariance violation on the θ_{23} and δ_{CP} measurements in T2K and NO ν A experiments are shown in Fig. 1. The standard fits on T2K and NO ν A data are illustrated with solid red and blue lines, respectively, whereas the fits obtained with Lorentz invariance violation are indicated with dashed lines. The discrepancy in the θ_{23} measurements is evident in the standard fits, which are clearly separated in T2K and NO ν A. This tension is partially removed with the introduction of LIV coefficient $\gamma_{\tau\tau}^{(5)}$. Imposing LIV into the fit leaves the T2K fit mostly unaffected but shifts the NO ν A fit significantly towards the θ_{23} value that is preferred by the T2K data. This results in an alleviation of tension in the T2K and NO ν A measurements. The tension between the T2K and NO ν A data can also be seen the fit results on δ_{CP} , which show nearly $\Delta\chi^2 \simeq 5$ difference at the value that is currently preferred by T2K data. Marginalizing over $\gamma_{\tau\tau}^{(D)}$ reduces this difference to $\Delta\chi^2 \simeq 2$. This amounts to about 1.8σ C.L. improvement.

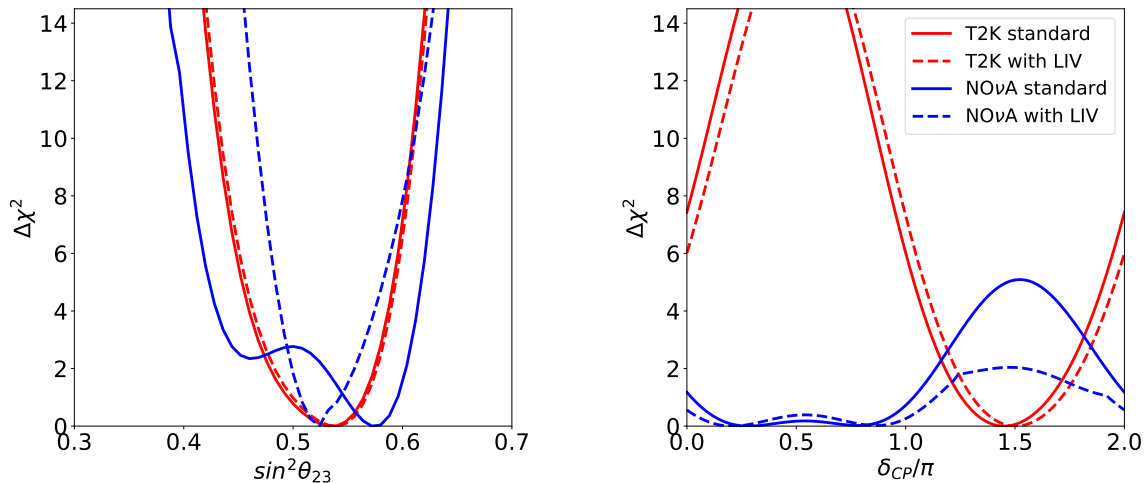


FIG. 1. The effect of Lorentz invariance violation on the determination of θ_{23} (left panel) and δ_{CP} (right panel) in T2K and NO ν A experiments. Fit results are shown for T2K and NO ν A experiments with red and blue lines, respectively. Solid lines correspond to the standard fit whereas dashed lines represent fit results where $\gamma_{\tau\tau}^{(5)}$ is taken as a free parameter.

The impact of each LIV parameter on the T2K and NO ν A analysis is further elaborated in Fig. 2. Each panel portrays the fit to $\delta_{CP} - \sin^2\theta_{23}$ plane as obtained from the joint analysis of the two experiments. The red curves represent the edges of the enclosed parameter space in the standard neutrino oscillations, as allowed by 90% C.L. in T2K and NO ν A. The best-fit point is marked with the red dot. On the other hand, the corresponding limits obtained with the freely-varying LIV parameters are presented with blue colour. The results show how the best-fit points shift upon the introduction of the single LIV coefficient for $D = 5$. The fits reveal that the best fit values for $\sin^2\theta_{23}$ and δ_{CP} shift significantly for parameters $\gamma_{\mu\mu}^{(D)}$ and $\gamma_{\tau\tau}^{(D)}$, whereas the inclusion of γ_{ee}^D , $\gamma_{e\mu}^D$ or $\gamma_{e\tau}^D$ only has notable effect on the fit value of δ_{CP} . The last off-diagonal parameter $\gamma_{\mu\tau}^D$ on the other hand leads to no significant changes in the fit values of $\sin^2\theta_{23}$ and δ_{CP} . The fit results obtained for dimensions $D = 4$ and 6 are analogous and are not shown here.

We finally make a remark on the effect of non-isotropic Lorentz invariance violation in neutrino experiments. As we pointed out in section II B, the recently measured anomalous muon magnetic moment [31] could be explained with non-isotropic LIV coefficient $d^{zt} = -1.7 \times 10^{-25}$. We investigated the potential effect of this solution in the long-baseline experiments T2K and NO ν A. Our results show non-isotropic coefficient too small to induce notable effects in T2K and NO ν A [59], where the value of d^{zt} required to satisfy $(g-2)_\mu$ leads only to $\chi_{\min}^2 \sim 10^{-3}$ correction to the fit result. It is

therefore possible to recover the measured $(g-2)_\mu$ value with non-isotropic LIV and alleviate the tension on θ_{23} in T2K and NO ν A at the same time.

V. CONCLUSIONS

Lorentz invariance violation could have profound effects in the interpretation of physical observations in laboratories and astrophysical environments. In the present work, we have investigated non-minimal LIV as a potential solution to the recently observed tension in the measurement of the atmospheric mixing angle θ_{23} and Dirac CP phase δ_{CP} in the long-baseline neutrino experiments T2K and NO ν A. To this extent, we interpreted the recently published experiment data in terms of isotropic and non-isotropic LIV effects.

In contrast to the previous studies conducted on the topic, we studied the relatively unexplored Lorentz invariance violation in dimensions $D = 4, 5$ and 6. Investigating the isotropic effect on the fits to T2K and NO ν A data, we found that diagonal parameters $\gamma_{\ell\ell'}^{(D)}$ ($\ell, \ell' = e, \mu$ and τ) could resolve the tension by about 0.4–2.4 σ confidence levels when one parameter is considered at a time. The extracted fit results are consistent with the existing bounds on Lorentz invariance violation in the neutrino sector [19]. We found the best fit with $\gamma_{\tau\tau}^{(5)} = 3.58 \times 10^{-32} \text{GeV}^{-1}$, which leads to an improvement of 2.41 σ C.L. from the standard scenario where Lorentz invariance remains conserved. In this case, the favoured values for the atmospheric mixing and Dirac CP phase are $\sin^2\theta_{23} = 0.526$ and $\delta_{CP} = 1.45\pi$, respectively.

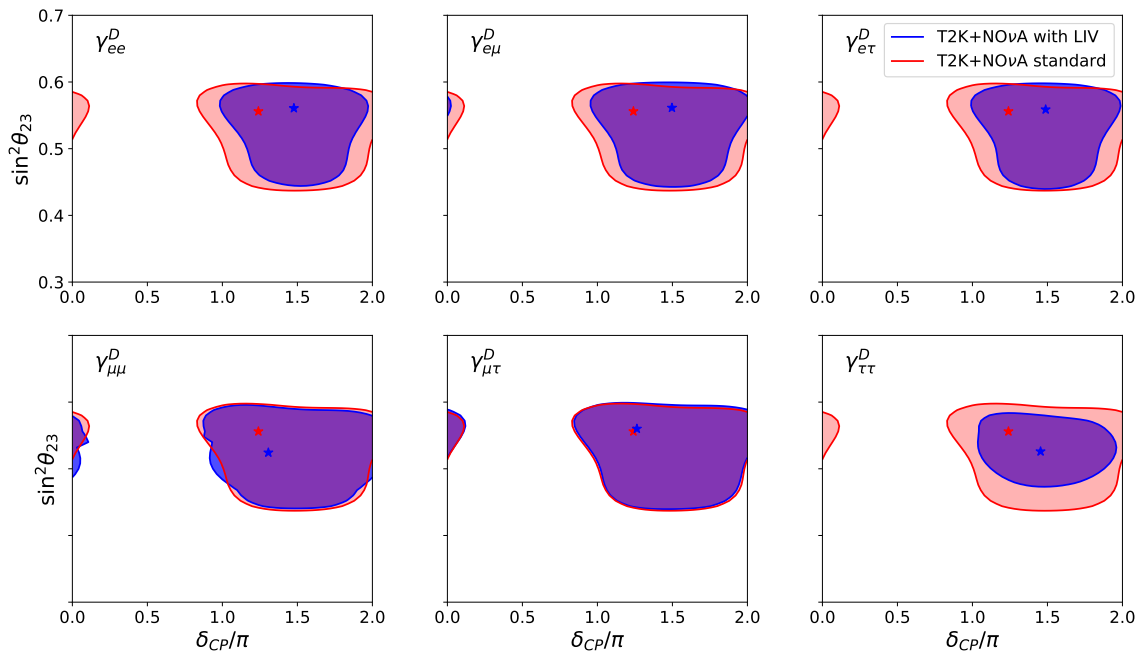


FIG. 2. Allowed values on the $\delta_{CP} - \sin^2 \theta_{23}$ plane according to the neutrino oscillation data in T2K and NO ν A experiments. Isotropic Lorentz invariance violation of dimension $D = 5$ is included in the parameter region highlighted with blue colour, whereas standard oscillations are shown with red colour. The best-fit values identified in the two scenarios are indicated with blue and red stars, respectively. The results are shown by 90% C.L. while assuming normally ordered neutrino masses.

Lorentz invariance violation is also able to explain the recent results on the anomalous muon magnetic moment as reported by the Muon $g - 2$ Collaboration [31]. The measured value of $(g - 2)_\mu$ could be generated by non-isotropic Lorentz invariance violation with directional coefficient $d^{zt} \simeq -1.7 \times 10^{-25}$. Isotropic Lorentz invariance violation on the other hand has no effect on the muon magnetic moment. We estimated the impact of this specific non-isotropic Lorentz invariance violation on the neutrino oscillations in T2K and NO ν A. We find the effect of the non-isotropic LIV parameter to be indistinguishable in T2K and NO ν A due to relatively small change in colatitude in their experimental setups. Though neutrino oscillations and muon $g - 2$ do not favour the same type of LIV, it is noteworthy that both solutions can exist simultaneously.

In summary, we have shown that non-minimal Lorentz invariance violation can notably alleviate the θ_{23} discrepancy in T2K and NO ν A data and simultaneously give rise to the anomalous muon magnetic moment. Respecting the present experimental bounds, we note that the significance for isotropic LIV can be as large as 2.41σ C.L. Our results place a mild preference on dimension-5 LIV. We are looking forward to the future long-baseline neutrino oscillation data to check whether the observed

discrepancy is due to the violation of Lorentz invariance.

ACKNOWLEDGMENTS

This project was supported in part by National Natural Science Foundation of China under Grant Nos. 12075326, 12090064, 11505301 and 11881240247. PP is additionally supported by the Shanghai Pujian Program under Grant No. 20PJ1407800 and SV by China Postdoctoral Science Foundation under Grant No. 2020M672930. JT and PP appreciate the support from CAS Center for Excellence in Particle Physics (CCEPP).

Appendix A: Implications on mass ordering

In the present work, we have conducted the analysis on T2K and NO ν A data assuming normal ordering for neutrino masses. For completeness, we now consider the results in the case of inverted ordering and discuss the implications on the sensitivity to neutrino mass ordering.

Figure 3 provides the fit results on the $\delta_{CP} - \sin^2 \theta_{23}$ plane at 90% C.L. in T2K and NO ν A experiments when

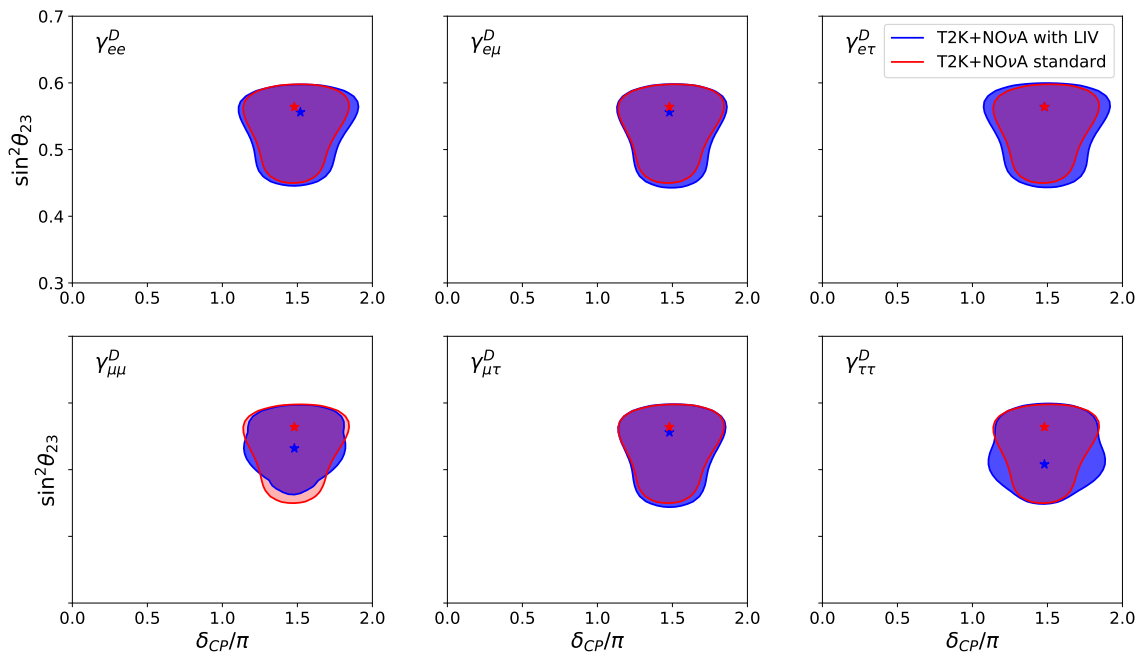


FIG. 3. Fit results on the $\delta_{CP} - \sin^2 \theta_{23}$ plane when inverted ordering is assumed. Neutrino data from the T2K and NO ν A experiments are analysed in the standard three-neutrino picture (red colour) and also letting $\gamma_{\ell\ell'}^{(D)}$ run free, whereby $D = 5$ and $\ell, \ell' = e, \mu$ and τ . Results are shown at 90% C.L. while the best-fit values are marked by stars.

inverted mass ordering is assumed. The standard three-neutrino oscillation scenario is taken into account in the red regions, which correspond to the scenario where no Lorentz invariance violation takes place. Isotropic LIV

is taken into account in the blue regions, which were obtained by letting $\gamma_{\ell\ell'}^{(D)}$ run free for $D = 5$ and $\ell, \ell' = e, \mu$ and τ . Each panel corresponds to the running of one

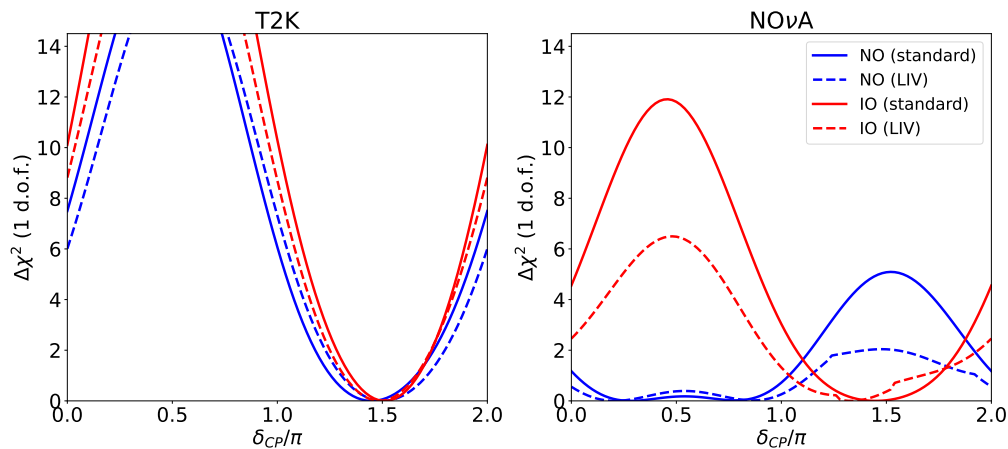


FIG. 4. The effect of Lorentz invariance violation on the determination of mass hierarchy in T2K and NO ν A. The fits to the far detector data in T2K (left panel) and NO ν A (right panel) are presented for normal ordering (NO) and inverted ordering (IO). In the standard scenario (solid) no violation is taken into account, while $\gamma_{\tau\tau}^{(5)}$ is marginalized in the LIV scenario (dashed).

LIV parameter, whilst other LIV parameters are fixed at zero. We have similarly performed the analysis for LIV parameters in dimensions $D = 4$ and 6, finding analogous results.

The effects of LIV is studied in the sensitivity to neutrino mass ordering by comparing the fit results in both neutrino mass orderings. The results are presented in Figure 4, where the fit results are shown separately for T2K and NO ν A in left and right panels, respectively. While the fit results associated with normal ordering (NO) are shown in blue colour, the results corresponding

to inverted ordering (IO) are indicated with red colour. The sensitivity to the neutrino mass ordering can be seen from the relative difference of $\Delta\chi^2$ between the NO and IO curves. In the standard oscillation scenario (solid curves), the difference between NO and IO is more significant in NO ν A than in T2K. The higher sensitivity in NO ν A arises mainly from the longer baseline length in the experiment. When the LIV effect is taken into account (dashed curves), the LIV parameter $\gamma_{\tau\tau}^{(5)}$ is let to vary freely. In such case, the difference between NO and IO is nearly halved for most values of δ_{CP} , indicating significant loss in mass hierarchy discrimination.

-
- [1] V. Alan Kostelecky and Robertus Potting, “Gravity from spontaneous Lorentz violation,” *Phys. Rev. D* **79**, 065018 (2009), arXiv:0901.0662 [gr-qc].
- [2] Marco Danilo Claudio Torri, “Neutrino Oscillations and Lorentz Invariance Violation,” *Universe* **6**, 37 (2020).
- [3] Vito Antonelli, Lino Miramonti, and Marco Danilo Claudio Torri, “Phenomenological Effects of CPT and Lorentz Invariance Violation in Particle and Astroparticle Physics,” *Symmetry* **12**, 1821 (2020).
- [4] Julian S. Schwinger, “The Theory of quantized fields. 1.” *Phys. Rev.* **82**, 914–927 (1951).
- [5] Gerhart Luders, “Proof of the TCP theorem,” *Annals Phys.* **2**, 1–15 (1957).
- [6] O. W. Greenberg, “CPT violation implies violation of Lorentz invariance,” *Phys. Rev. Lett.* **89**, 231602 (2002), arXiv:hep-ph/0201258.
- [7] V. Alan Kostelecky and Stuart Samuel, “Spontaneous Breaking of Lorentz Symmetry in String Theory,” *Phys. Rev. D* **39**, 683 (1989).
- [8] V. Alan Kostelecky and Robertus Potting, “CPT and strings,” *Nucl. Phys. B* **359**, 545–570 (1991).
- [9] M. S. Berger and V. Alan Kostelecky, “Supersymmetry and Lorentz violation,” *Phys. Rev. D* **65**, 091701 (2002), arXiv:hep-th/0112243.
- [10] Patricio Gaete, J. A. Helayël-Neto, and Alessandro D. A. M. Spallicci, “Aspects of Lorentz-Poincaré-symmetry violating physics in a supersymmetric scenario,” (2021), arXiv:2104.06875 [hep-ph].
- [11] Gabriela Barenboim and Joseph D. Lykken, “A Model of CPT Violation for Neutrinos,” *Phys. Lett. B* **554**, 73–80 (2003), arXiv:hep-ph/0210411.
- [12] Don Colladay and V. Alan Kostelecky, “Lorentz violating extension of the standard model,” *Phys. Rev. D* **58**, 116002 (1998), arXiv:hep-ph/9809521.
- [13] Gaurav Tomar, Subhendra Mohanty, and Sandip Pakvasa, “Lorentz Invariance Violation and IceCube Neutrino Events,” *JHEP* **11**, 022 (2015), arXiv:1507.03193 [hep-ph].
- [14] Floyd W. Stecker, “Testing Lorentz Symmetry using High Energy Astrophysical Observations,” *Symmetry* **9**, 201 (2017), arXiv:1708.05672 [astro-ph.HE].
- [15] Jun-Jie Wei, Bin-Bin Zhang, Lang Shao, He Gao, Ye Li, Qian-Qing Yin, Xue-Feng Wu, Xiang-Yu Wang, Bing Zhang, and Zi-Gao Dai, “Multimessenger tests of Einstein’s weak equivalence principle and Lorentz invariance with a high-energy neutrino from a flaring blazar,” *JHEAp* **22**, 1–4 (2019), arXiv:1807.06504 [astro-ph.HE].
- [16] Ushak Rahaman, “Looking for Lorentz invariance violation (LIV) in the latest long baseline accelerator neutrino oscillation data,” *Eur. Phys. J. C* **81**, 792 (2021), arXiv:2103.04576 [hep-ph].
- [17] Ziming Wang, Lijing Shao, and Chang Liu, “New limits on the Lorentz/CPT symmetry through fifty gravitational-wave events,” (2021), arXiv:2108.02974 [gr-qc].
- [18] Sidney R. Coleman and Sheldon L. Glashow, “High-energy tests of Lorentz invariance,” *Phys. Rev. D* **59**, 116008 (1999), arXiv:hep-ph/9812418.
- [19] V. Alan Kostelecky and Neil Russell, “Data Tables for Lorentz and CPT Violation,” (2008), arXiv:0801.0287 [hep-ph].
- [20] Ivan Esteban, M. C. Gonzalez-Garcia, Michele Maltoni, Thomas Schwetz, and Albert Zhou, “The fate of hints: updated global analysis of three-flavor neutrino oscillations,” *JHEP* **09**, 178 (2020), arXiv:2007.14792 [hep-ph].
- [21] A. Aguilar-Arevalo *et al.* (LSND), “Evidence for neutrino oscillations from the observation of $\bar{\nu}_e$ appearance in a $\bar{\nu}_\mu$ beam,” *Phys. Rev. D* **64**, 112007 (2001), arXiv:hep-ex/0104049.
- [22] Carlo Giunti and Marco Laveder, “Statistical Significance of the Gallium Anomaly,” *Phys. Rev. C* **83**, 065504 (2011), arXiv:1006.3244 [hep-ph].
- [23] G. Mention, M. Fechner, Th. A. Mueller, D. Lhuillier, M. Cribier, and A. Letourneau, “The Reactor Antineutrino Anomaly,” *Phys. Rev. D* **83**, 073006 (2011), arXiv:1101.2755 [hep-ex].
- [24] A. A. Aguilar-Arevalo *et al.* (MiniBooNE), “Significant Excess of ElectronLike Events in the MiniBooNE Short-Baseline Neutrino Experiment,” *Phys. Rev. Lett.* **121**, 221801 (2018), arXiv:1805.12028 [hep-ex].
- [25] Tommy Ohlsson, “Status of non-standard neutrino interactions,” *Rept. Prog. Phys.* **76**, 044201 (2013), arXiv:1209.2710 [hep-ph].
- [26] Peter B. Denton, Julia Gehrlein, and Rebekah Pestes, “ CP -Violating Neutrino Nonstandard Interactions in Long-Baseline-Accelerator Data,” *Phys. Rev. Lett.* **126**, 051801 (2021), arXiv:2008.01110 [hep-ph].
- [27] Zhuojun Hu, Jiajie Ling, Jian Tang, and TseChun Wang, “Global oscillation data analysis on the 3ν mixing without unitarity,” *JHEP* **01**, 124 (2021), arXiv:2008.09730 [hep-ph].
- [28] Basudeb Dasgupta and Joachim Kopp, “Sterile Neutri-

- nos,” Phys. Rept. **928**, 1–63 (2021), arXiv:2106.05913 [hep-ph].
- [29] K. Abe *et al.* (T2K), “Improved constraints on neutrino mixing from the T2K experiment with 3.13×10^{21} protons on target,” Phys. Rev. D **103**, 112008 (2021), arXiv:2101.03779 [hep-ex].
- [30] M. A. Acero *et al.* (NOvA, R. Group), “An Improved Measurement of Neutrino Oscillation Parameters by the NOvA Experiment,” (2021), arXiv:2108.08219 [hep-ex].
- [31] B. Abi *et al.* (Muon $g-2$), “Measurement of the Positive Muon Anomalous Magnetic Moment to 0.46 ppm,” Phys. Rev. Lett. **126**, 141801 (2021), arXiv:2104.03281 [hep-ex].
- [32] Andrew G. Cohen and Sheldon L. Glashow, “A Lorentz-Violating Origin of Neutrino Mass?” (2006), arXiv:hep-ph/0605036.
- [33] Alan Kostelecky and Matthew Mewes, “Neutrinos with Lorentz-violating operators of arbitrary dimension,” Phys. Rev. D **85**, 096005 (2012), arXiv:1112.6395 [hep-ph].
- [34] Vito Antonelli, L. Miramonti, and M. D. C. Torri, “Neutrino oscillations and Lorentz Invariance Violation in a Finslerian Geometrical model,” Eur. Phys. J. C **78**, 667 (2018), arXiv:1803.08570 [hep-ph].
- [35] V. Alan Kostelecky and Matthew Mewes, “Lorentz and CPT violation in neutrinos,” Phys. Rev. D **69**, 016005 (2004), arXiv:hep-ph/0309025.
- [36] The full derivation of equation (7) can be found in Appendix A of Ref. [35].
- [37] Colatitude is expressed as complement of latitude, that is, $\Phi = \pi - \Theta$.
- [38] Robert Bluhm, V. Alan Kostelecky, and Charles D. Lane, “CPT and Lorentz tests with muons,” Phys. Rev. Lett. **84**, 1098–1101 (2000), arXiv:hep-ph/9912451.
- [39] André H. Gomes, Alan Kostelecký, and Arnaldo J. Vargas, “Laboratory tests of Lorentz and CPT symmetry with muons,” Phys. Rev. D **90**, 076009 (2014), arXiv:1407.7748 [hep-ph].
- [40] Alexander Keshavarzi (Muon $g-2$), “The Muon $g - 2$ Experiment at Fermilab,” EPJ Web Conf. **212**, 05003 (2019), arXiv:1905.00497 [hep-ex].
- [41] Michel Davier, Andreas Hoecker, Bogdan Malaescu, and Zhiqing Zhang, “Reevaluation of the Hadronic Contributions to the Muon $g-2$ and to $\alpha(m_Z^2)$,” Eur. Phys. J. C **71**, 1515 (2011), [Erratum: Eur.Phys.J.C 72, 1874 (2012)], arXiv:1010.4180 [hep-ph].
- [42] Gilberto Colangelo, Martin Hoferichter, Massimiliano Procura, and Peter Stoffer, “Rescattering effects in the hadronic-light-by-light contribution to the anomalous magnetic moment of the muon,” Phys. Rev. Lett. **118**, 232001 (2017), arXiv:1701.06554 [hep-ph].
- [43] Michel Davier, Andreas Hoecker, Bogdan Malaescu, and Zhiqing Zhang, “Reevaluation of the hadronic vacuum polarisation contributions to the Standard Model predictions of the muon $g - 2$ and $\alpha(m_Z^2)$ using newest hadronic cross-section data,” Eur. Phys. J. C **77**, 827 (2017), arXiv:1706.09436 [hep-ph].
- [44] M. Davier, A. Hoecker, B. Malaescu, and Z. Zhang, “A new evaluation of the hadronic vacuum polarisation contributions to the muon anomalous magnetic moment and to $\alpha(m_Z^2)$,” Eur. Phys. J. C **80**, 241 (2020), [Erratum: Eur.Phys.J.C 80, 410 (2020)], arXiv:1908.00921 [hep-ph].
- [45] T. Aoyama *et al.*, “The anomalous magnetic moment of the muon in the Standard Model,” Phys. Rept. **887**, 1–166 (2020), arXiv:2006.04822 [hep-ph].
- [46] K. Abe *et al.* (T2K), “T2K measurements of muon neutrino and antineutrino disappearance using 3.13×10^{21} protons on target,” Phys. Rev. D **103**, L011101 (2021), arXiv:2008.07921 [hep-ex].
- [47] K. Abe *et al.* (T2K), “Constraint on the matter–antimatter symmetry-violating phase in neutrino oscillations,” Nature **580**, 339–344 (2020), [Erratum: Nature 583, E16 (2020)], arXiv:1910.03887 [hep-ex].
- [48] Patrick Huber, M. Lindner, and W. Winter, “Simulation of long-baseline neutrino oscillation experiments with GLOBES (General Long Baseline Experiment Simulator),” Comput. Phys. Commun. **167**, 195 (2005), arXiv:hep-ph/0407333.
- [49] Patrick Huber, Joachim Kopp, Manfred Lindner, Mark Rolinec, and Walter Winter, “New features in the simulation of neutrino oscillation experiments with GLOBES 3.0: General Long Baseline Experiment Simulator,” Comput. Phys. Commun. **177**, 432–438 (2007), arXiv:hep-ph/0701187.
- [50] G. L. Fogli, E. Lisi, A. Marrone, D. Montanino, and A. Palazzo, “Getting the most from the statistical analysis of solar neutrino oscillations,” Phys. Rev. D **66**, 053010 (2002), arXiv:hep-ph/0206162.
- [51] S. V. Cao (T2K), “Latest results from T2K,” in *53rd Rencontres de Moriond on Electroweak Interactions and Unified Theories* (2018) arXiv:1805.05917 [hep-ex].
- [52] K. Abe *et al.* (T2K), “Search for CP Violation in Neutrino and Antineutrino Oscillations by the T2K Experiment with 2.2×10^{21} Protons on Target,” Phys. Rev. Lett. **121**, 171802 (2018), arXiv:1807.07891 [hep-ex].
- [53] Jeremy Hewes, “Recent searches for sterile neutrinos in NOvA,” A talk presented at NuFact 2021, <https://indico.cern.ch/event/855372/contributions/4450790/>, accessed: Oct 7th, 2021.
- [54] Mark D. Messier, *Evidence for neutrino mass from observations of atmospheric neutrinos with Super-Kamiokande*, Ph.D. thesis, Boston U. (1999).
- [55] E. A. Paschos and J. Y. Yu, “Neutrino interactions in oscillation experiments,” Phys. Rev. **D65**, 033002 (2002), hep-ph/0107261.
- [56] M. G. Aartsen *et al.* (IceCube), “Neutrino Interferometry for High-Precision Tests of Lorentz Symmetry with IceCube,” Nature Phys. **14**, 961–966 (2018), arXiv:1709.03434 [hep-ex].
- [57] S. S. Wilks, “The Large-Sample Distribution of the Likelihood Ratio for Testing Composite Hypotheses,” Annals Math. Statist. **9**, 60–62 (1938).
- [58] Sara Algeri, Jelle Aalbers, Knut Dundas Morã, and Jan Conrad, “Searching for new phenomena with profile likelihood ratio tests,” Nature Rev. Phys. **2**, 245–252 (2020), arXiv:1911.10237 [physics.data-an].
- [59] The smallness of the non-isotropic effect is mainly owed to the relatively small difference in colatitudes between T2K and NOvA. In T2K, colatitude is given by $\cos \Theta = 0.993$ whereas in NOvA it is $\cos \Theta = 1.000$. Future experiments with longer baseline lengths could see more profound effect from non-isotropic Lorentz invariance violation.